ISSN 1069-3513, Izvestiya, Physics of the Solid Earth, 2011, Vol. 47, No. 7, pp. 610–622. © Pleiades Publishing, Ltd., 2011.
Original Russian Text © M.G. Potanina, V.B. Smirnov, P. Bernard, 2011, published in Fizika Zemli, 2011, No. 7, pp. 54–66.

Patterns of Seismic Swarm Activity in the Corinth Rift in 2000–2005

M. G. Potanina[a,b], **V. B. Smirnov**[a,b], **and P. Bernard**[c]

[a] *Faculty of Physics, Moscow State University, Moscow, Russia*

[b] *Schmidt Institute of Physics of the Earth, Russian Academy of Sciences, ul. Bol'shaya Gruzinskaya 10, Moscow, 123995 Russia*

[c] *Institute de Physique du Globe de Paris, Paris, France*

Received February 7, 2011

Abstract—Based on the data of the detailed earthquake catalog provided on the website of the Corinth Rift Laboratory, zones of swarm activity are revealed and the variations in the statistical parameters of seismic swarms that occurred in the western part of the Gulf of Corinth are calculated. The preliminary analysis of the catalogue is carried out; the magnitude of completeness and the accuracy of the location of the earthquake are estimated; the changes in these parameters associated with the development of the observational network are assessed. The *b*-value (*b*-values) and the cluster dimension of the set of hypocenters are estimated, and time variations in these parameters in the course of the evolution of swarm activity are revealed. The style of changes in the parameters characterizing the seismic regime during intervals of swarm activity indicates that the process of failure exhibits scale redistribution over the course of time, changing from upscaling (progression from smaller to larger scales) at the stage of increasing seismicity to downscaling (progression from larger to lower scales) at the stage of decay. These particular features of enhancement and reduction of swarm seismicity are qualitatively similar to the scenarios of source preparation and aftershock relaxation of strong earthquakes. The pattern of variations of the swarm seismicity studied is similar to those identified in the previous laboratory and field modeling of various transient modes of seismicity. This fact confirms the relevancy of the retrieved results and conclusions based on the laboratory studies of transient modes, and suggests that the latter have a universal governing mechanism.

DOI: 10.1134/S106935131106005X

INTRODUCTION

The laboratory and field modeling of transient seismic processes revealed the specific changes that occur in the statistical parameters of the seismic regime in the course of evolution of seismic activity induced by external impacts [Smirnov et al., 2010]. In particular, it was found in laboratory experiments on the initiation of swarm-like activity that the Gutenberg–Richter *b*-value varies in time: it decreases during the excitation of swarm seismicity and increases at the stage of decay. The value of this effect, measured in terms of the depth of the minimum in the *b*-value, increased with the increasing level of stresses at which the initiation took place. Similar variations in the *b*-value were detected in the field experiment on the initiation of microseismicity by water injection in a borehole.

The change in the *b*-value, which was revealed in the experiments, means that the time variations in the activity are different on different scales of the process (in different energy ranges), that is, the redistribution of the failure over the scales occurs. The decrease in the *b*-value during increased activity indicates that the share of strong events increases with time; that is, the process of failure develops from lower to higher scales. Decay in activity is associated with the opposite situation: the share of strong events decreases over time, and the failure process develops from larger to smaller scales.

The scenarios of the development of a failure with redistribution over scales are known in the theory of a seismic regime. Transition from smaller to larger scales (upscaling) is typical for the processes of earthquake preparation. This transition is associated with fusion of cracks located nearby and, correspondingly, with a higher percentage of large cracks. This scenario, which has been repeatedly addressed in the literature, lays the physical basis for the concept of the avalanche unstable fracture (AUF) [Sobolev, 1993]. The downscaling transition (from larger to smaller scales) is recognized in the aftershock sequences [Smirnov and Ponomarev, 2004]. In [Smirnov et al., 2010], it was supposed that these scenarios are universal for different transient seismic modes. In order to verify this supposition, in the present paper we analyze variations of the seismic regime for two natural seismic swarms in the Corinth Rift.

THE CORINTH RIFT

The Corinth Rift located in the western part of Central Greece is one of the most active European seismic zones. During the past thirty-five years, this region has been hit by five earthquakes with a magnitude in excess of 5.8, some of which resulted in disastrous historical events. Seismic swarms also frequently occur in this region [Bernard et al., 2006]. The spreading rate of the rift is estimated at 1–1.5 cm per annum. These features are believed to be due to the complex distribution of crustal deformations in the region, which include an extension of the Aegean Sea on the east and a zone of subduction in the south where the African plate subsides under the Eurasian plate [Ford et al., 2007; Lykousis et al., 2006]. This tectonic pattern is responsible for the asymmetry of the rift: the most active normal fault dips north, which causes the northern coast to slowly subside and the displacement of the coasts of the rift to increase. The displacement rate is different in different parts of the region: in the western segment of the Gulf of Corinth, according to GPS data, it measures 14 mm per annum, while in the eastern segment it is about 10 mm per annum [Bourouis and Cornet, 2009]. The stratigraphic pattern follows the tectonic situation: the northern part of the gulf is framed by mountains covered by limestone while in the southern part there are conglomerates with exposed rocks on the coasts of the southern active faults [Bernard et al., 2006]. The pattern of seismicity in the western and eastern segments of the rift is also different. The western part of the region is characterized by frequently occurring swarms of microearthquakes with magnitudes below 4.5. The eastern segment is hit by rare but much stronger quakes [Bourouis and Cornet, 2009].

Detailed field observations of microseismic activity have been launched by the deployment in 1999 of a temporary seismic network near the town of Aigion, approximately 40 km to the east of the town of Pathra. These observations revealed a seismically active zone three to four kilometers thick. According to [Rietbork et al., 1996; Bernard et al., 1997; Bourouis and Cornet, 2009], this shallow zone gently dips (at about 20°) north from a depth of 5–8 km on the southern coast to 9–12 km near the northern coast. In [Rigo et al., 1996], this zone was interpreted as a detachment zone, on which "the major north-dipping normal faults are rooting, and which acts as a shear zone controlling the fault pattern of the rift" [Bernard et al., 2006].

At the same time, in parallel with the seismic measurements, continuous GPS observations [Avalone et al., 2004] have been conducted for eleven years. These measurements provided the data to characterize the process of the deformation on a regional scale. It was shown that the spreading rate in the central and western part of the rift is 11 and 16 mm per year, respectively.

Normal faults in the western part of the rift are confined to a surface that dips north at 60°, which gave rise to a suggestion of the probable correlation of the seismogenic zone with these cascade dipping faults. In [Briole et al., 2000; Bernard et al., 2006], it was supposed that the dip angles of the faults do not vary with depth; however, the fault zone terminates by the detachment zone located near the base of the seismogenic zone. At the same time, the detailed seismic observations and offshore bathymetry to the east of the town of Aigion revealed south-dipping normal faults close to the northern coast of the rift [McNeil et al., 2005; Bell et al., 2009].

In 1999, in the area of Aigion in the western part of the Gulf of Corinth, a multipurpose observatory known as the Corinth Rift Laboratory was established[1] The main goal of CRL was to study in situ the mechanics of active faults and, in particular, the pattern of their quasi-static and dynamical interaction with a special emphasis on the role of the fluids [Henry and Moretti, 2006; Bernard et al., 2006; Bourouis and Cornet, 2009].

Over eight years of continuous measurements, more than 30000 earthquakes with a magnitude above 0.5 have been recorded. The seismic swarms of 2001 and 2003–2004, which are considered in the present paper, are discussed in detail in [Lyon-Caen et al., 2004; Pacchiani and Lyon-Caen, 2009; Bourouis and Cornet, 2009]. During the swarm activity of 2001, a relatively strong earthquake with a magnitude of 4.2 occurred within the swarm. The swarm of 2003–2004 was not accompanied by anomalous seismic events. The emergence of swarms is believed to be associated with the diffusion of a fluid through a complex system of fractures in a seismogenic zone [Bourouis and Cornet, 2009].

INITIAL DATA

The original data for our study were taken from the CRL catalogue for the period from May 23, 2000 through March 21, 2006. The catalogue for this interval contains information on 35122 seismic events with $M \geq 0.2$. The magnitudes in the catalogue are moment magnitudes.

At the first stage of processing, we carried out the preliminary analysis of the catalogue in order to assess the uniformity and completeness of the data.

The evaluation of the magnitudes of completeness is based on the concept of the power-law energy distribution of earthquakes; in this case, the log-log plot of the magnitude-frequency dependence is a straight line. If, however, a part of earthquakes is missed, the points for the corresponding magnitudes will fall below the curve of the frequency-magnitude dependency, which defines the well-known effect of the "bending" of the frequency-magnitude relation in small magnitudes. In terms of statistics, the problem of finding the magnitude of completeness is reduced to the question of whether the observed distribution of earthquakes over energy obeys the power law. Such a statement of the statistical problem has been formulated and solved in [Pisarenko, 1989; Sadovskii and

[1] For details, visit the CRL website at http://crlab.eu.

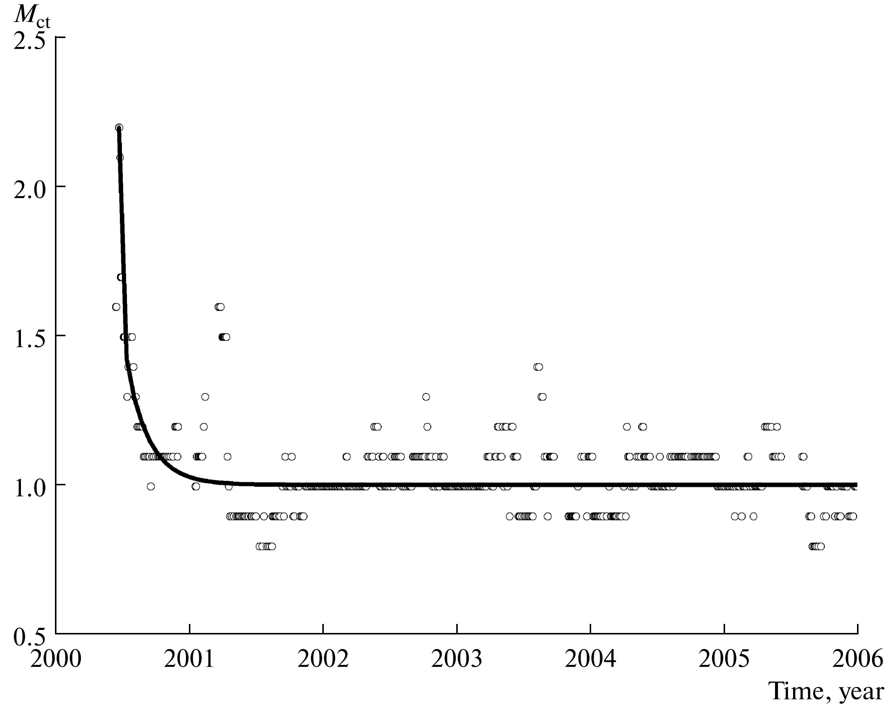

Fig. 1. Time variations of the magnitude of completeness.

Pisarenko, 1991]. V.F. Pisarenko provided a strict solution, which allows one to computerize the entire procedure of the analysis by only specifying the level of significance for testing the corresponding hypotheses.

The program implementation of the procedure of assessing the magnitude of completeness renders estimation in spatio-temporal bins that move in the space-time domain with a step specified by the user. This allows obtaining information on space and time variations in the magnitude of completeness [Smirnov, 1997; 2009].

The spatial distribution of the magnitude of completeness is beyond the scope of the present work. The time variations of the magnitude of completeness M_{ct} for the entire region are depicted in Fig. 1 (estimation was carried out in a moving time window with a length of 0.1 year and a shift of 0.01 year). A noticeable decrease of the magnitude of completeness within first few months of the network's operation is likely due to the gradual attainment of the stable mode of the network's operation. The anomalous spikes in M_{ct} that reach a level of 1.4–1.5 at the beginning of 2001 and at the end of 2003 correspond to the times of seismic swarms. This impairment in completeness is probably associated with the sharply increased (by an order of magnitude) number of seismic events and corresponding overloading of the network. A similar effect was observed in the aftershock sequences [Smirnov, 1997]. In the further analysis of the swarm's activity, the magnitude of completeness was estimated separately for every individual swarm.

The uncertainties in the location of hypocenters of microearthquakes are not indicated in the catalogue used. These uncertainties can be estimated if we turn to the concept of the fractal geometry of seismicity. For a fractal set of points, the distance between them obeys the power law [Mandelbrot, 2002; Feder, 1991]. Therefore, the log-log plot of this distribution should be a straight line. In the case of real objects, linearity is observed in a certain interval of distances known as the scaling range (in the terminology of [Mandelbrot, 2002], the limiting values of the scaling range are referred to as the inner and outer cutoffs). In the case of seismicity, the outer cutoff is typically determined by the size of a cluster of events or by the size of a region covered by the catalogue, while the inner cutoff is defined by the error of the earthquake location. Thus, by estimating the lower threshold of scaling, we can assess the effective accuracy of the location of the earthquake.

The most common approach in estimating the fractal properties of seismicity is the method of the correlation integral. The latter is an estimate of the distribution function of distances between earthquakes (see below). Figure 2 presents the graphs of correlation integrals for the sets of epicenters and hypocenters of earthquakes, calculated for successive time intervals (only the graphs for the starting part of the catalogue in windows containing 150 events are shown in the fig-

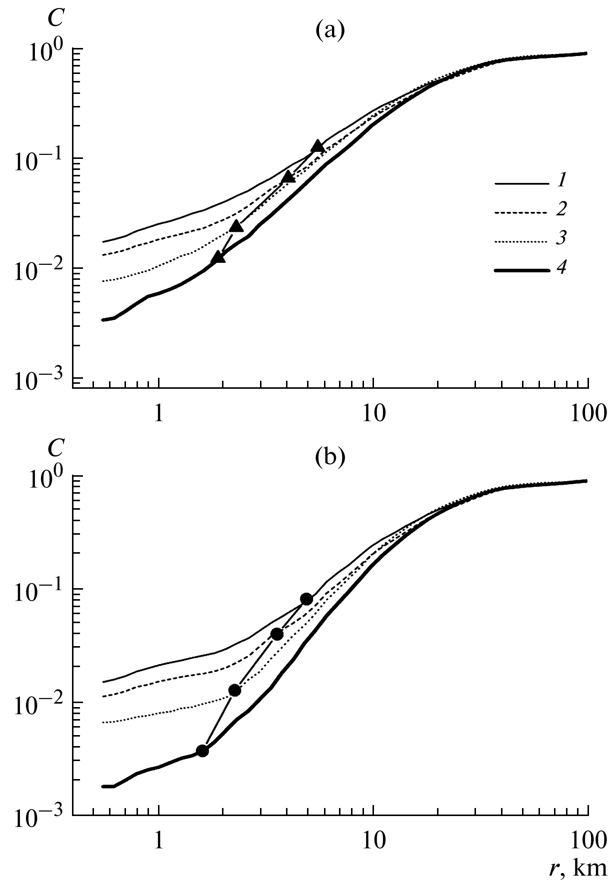

Fig. 2. A family of correlation integrals for a set of (a) epicenters and (b) hypocenters in different time periods: *1* – 2000.50, *2* – 2000.51, *3* – 2000.60, *4* – 2001.00. The inner cutoffs of the scaling range are marked by triangles and circles.

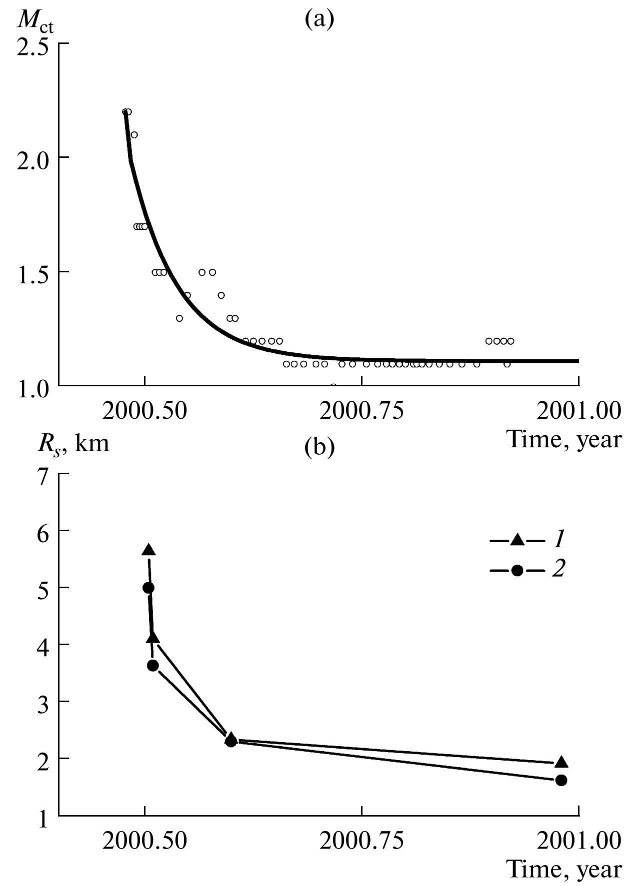

Fig. 3. Time variations of the (a) magnitude of completeness and (b) error of location for a period of 2001. *1* the epicenter location error, *2* is the inner cutoff of the scaling range.

ure). The upper boundary of the scaling interval is almost similar for different time segments and amounts to 20–30 km, which is determined by the size of the seismogenic area covered by the catalogue. The lower scaling limit, which is indicated by bold markers in Fig. 2, decreases over the course of time. Its time dependence for the initial part of the catalogue is presented in Fig. 3b. Figure 3a shows how the magnitude of completeness changes in time (the initial part of the curve in Fig. 1). It is seen in Fig. 3 that the inner cutoff decreases synchronously with the decrease in the magnitude of completeness. This fact supports the interpretation of the inner cutoff as an effective error of the location of the earthquake sources: the decreasing magnitude of completeness reflects the increasing accuracy of the seismic network, which is accompanied by the decreasing errors of the location of seismic events. According to the data presented in Fig. 3, as the network attained a stable mode of operation, the location error was 1–2 km. The analysis of correlation integrals showed that this value has not changed significantly since 2001.

AREAS OF SEISMIC SWARMS

For selecting the catalogue events that relate to the seismic swarms of 2001 and 2003–2004, we used the published data [Lyon-Caen et al., 2004; Pacchiani and Lyon-Caen, 2009; Bourouis and Cornet, 2009] and our own estimates of spatiotemporal density of earthquake distribution. The density was calculated using the software intended for studying the RTL parameter [Sobolev et al., 2009] that provides the maps of distributions of weighted seismic activity in successive time intervals. The weighting coefficients and the parameters of spatiotemporal windows were fitted empirically. The results of the identification of the swarms are shown in Fig. 4.

The swarm of 2001 is clustered in the continental part of the region. It contains a relatively strong earthquake with $M = 4.2$ that occurred on April 8, 2001, seventy days after the onset of the swarm activity. The magnitude of completeness within this swarm is $M_{ct} = 1.4$, and, for the purposes of our analysis, the catalogue has been selected according to this value.

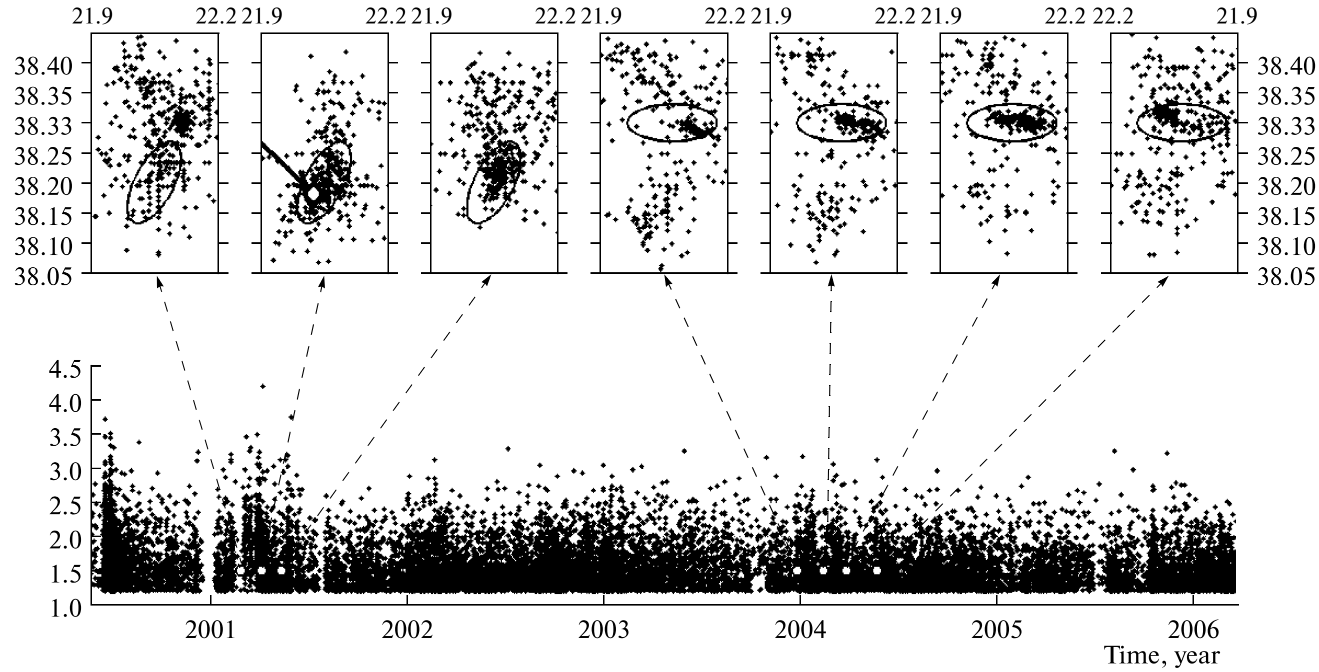

Fig. 4. Maps of seismicity in the western part of the Corinth rift for different time periods. The areas of swarms are outlined by ovals. The time diagram shows the magnitudes of the earthquakes; the timing of the maps is indicated by arrows. For the swarm of 2001, the location of the epicenter of $M = 4.2$ earthquake of April 8, 2001 is plotted.

The swarm of 2003–2004 relates to the oceanic region and does not contain any earthquakes with anomalous magnitudes. Estimation of the magnitude of completeness gives $M_{ct} = 1.2$; however, in order to provide compatibility of the results of analysis for both swarms, the catalogue for 2003–2004 has also been selected by the same criterion of $M_{ct} = 1.4$ as the catalogue for the swarm of 2001.

THE STATISTICAL PARAMETERS

To analyze the seismic regime of the selected swarms, a number of statistical parameters were estimated in the moving time windows. These parameters are described below, and those of them which are uncommon are considered in more detail.

***b*-value (the slope of the frequency–magnitude diagram.)** Normally, the b-value is assessed using the maximum likelihood estimate for an ungrouped sample [Kendal and Stewart, 1973]:

$$b = \frac{\log e}{\bar{M} - M_0}, \tag{1}$$

where $\bar{M}$ is the average magnitude and M_0 is the minimal magnitude across the sample (in our case, it is the magnitude of completeness of the catalogue). The uncertainty of the estimate of the b-value was calculated as a square root of the asymptotical variance, which is equal to b^2/N: $S_b = b/\sqrt{N}$, where N is the number of events.

As seen from (1), the b-value is, in fact, inverse to the average magnitude estimated over the given sample of events. In the case of a right-censored sample (i.e., when the events with the magnitudes that exceed a certain threshold are excluded from the sample for some reason), the average magnitude is underestimated with respect to the true mean value, and, correspondingly, the b-value determined by Eq. (1) is overestimated. For example, the b-value estimated from the samples of different lengths that belong to one and the same general population (a model example), exhibits a systematic discrepancy: the shorter the sample, the narrower the interval of magnitudes of events that fall in this interval, and the smaller the estimate of the average magnitude, the smaller the b-value calculated according to formula (1). In seismic applications, censoring is necessary when the length of the time window is insufficient for estimating the frequency of recurrence of rather strong events. This situation is observed when the probability for the event of a given magnitude to occur within the time interval considered (which is equal to the length of the time window) is far less then unity.

The maximum likelihood estimate (MLE) of the b-value for a censored sample is easy to derive.

For a censored exponential distribution with parameter α,

$$p = \frac{\alpha e^{\alpha X_1}}{1 - e^{-\alpha(X_2 - X_1)}} e^{-\alpha x}, \quad x \in [X_1, X_2]$$

the logarithmic likelihood function has the following form:

$$\ln L = N\ln\alpha + N\alpha X_1 - \alpha\sum_{i=1}^{N} x_i - N\ln\left(1 - e^{-\alpha(X_2 - X_1)}\right).$$

Its derivative is

$$\frac{\partial \ln}{\partial \alpha} = \frac{N}{\alpha} - N\frac{\Delta X}{e^{\alpha\Delta X} - 1} - \frac{N}{\alpha_0},$$

where $\Delta X = X_2 - X_1$ and $\frac{1}{\alpha_0} = \frac{1}{N}\sum_{i=1}^{N} x_i - X_1$.

MLE for α is obtained from the condition $\frac{\partial \ln L}{\partial \alpha} = 0$:

$$\frac{1}{\alpha} = \frac{1}{N}\sum_{i=1}^{N} x_i - X_1 + \frac{\Delta X}{e^{\alpha\Delta X} - 1} = \frac{1}{\alpha_0} + \frac{\Delta X}{e^{\alpha\Delta X} - 1}. \quad (2)$$

Solution to Eq. (2) yields MLE for α.

To estimate the variance of α, the second derivative of the likelihood function is required:

$$\frac{\partial^2 \ln L}{\partial \alpha^2} = -N\left(\frac{1}{\alpha^2} - \left(\frac{\Delta X}{e^{\alpha\Delta X} - 1}\right)^2 e^{\alpha\Delta X}\right)$$
$$= -\frac{N}{\alpha^2}\left(1 - \left(\frac{\alpha\Delta X}{e^{\alpha\Delta X} - 1}\right)^2 e^{\alpha\Delta X}\right).$$

Then,

$$S_\alpha = \sqrt{\left(-\frac{\partial^2 \ln L}{\partial \alpha_2}\right)} = \frac{\alpha}{\sqrt{N}}\frac{1}{\sqrt{1 - \left(\frac{\alpha\Delta X}{e^{\alpha\Delta X} - 1}\right)^2 e^{\alpha\Delta X}}}. \quad (3)$$

The distribution of magnitudes (the Gutenberg–Richter law) has the form

$$p \sim 10^{-bM} = e^{-bM\ln 10}.$$

Therefore, in Eqs. (2) and (3), we must set $x = M$, calculate α, S_α, and obtain b and S_b as

$$b = \alpha/\ln 10 \quad (4)$$

and

$$S_b = S_\alpha/\ln 10. \quad (5)$$

The difference between the estimates (4) and (1) is considerable when $\Delta M = M_2 - M_1 < 2$; the error of (5) in this case is severalfold larger than the error of (1).

When estimating the b-value for a sample in a given time window, it is unclear by which value of magnitude the sample should be censored, because there is no a priori information about the probability of the occurrence of seismic events with different magnitudes. An approximate approach in this situation is probably to censor the sample by the value M_2 of the strongest event across the sample. This is a rather severe requirement, because the use of Eqs. (4) and (5) in this case implies *the impossibility* of seismic events with magnitudes in excess of M_2 to occur within the selected time interval. However, the unknown probability of such events is actually not zero. Thus, when using MLE for a sample censored by a strongest event, we underestimate the b-value compared to its true value.

Based on the above, when assessing the b-value for relatively small samples, the expression (1) will be regarded as the right estimate, and expression (4), as the left estimate.

***d*-value (fractal dimension of a set of hypocenters).** The fractal dimension was estimated by the correlation integral

$$C(r) = \frac{n(\Delta r \le r)}{N_0},$$

where $n(\Delta r \le r)$ is the number of all possible pairs of events spaced apart from each other by Δr that is at most r, and N_0 is the total number of all possible pairs of events. For fractal sets, $C(r) \sim r^d$, where d is the correlation fractal dimension. The correlation integral is based on the statistics of all possible pairs of events, the number of which is rather large even for small samples (the number of all possible pairs of events in a sample containing N events is $N_0 = N(N-1)/2$). This makes the estimate of the correlation dimension rather stable in the case of small samples; however, on the other hand, it is difficult to estimate the confidence interval here. The set of $N(N-1)/2$ distances between all possible pairs, which is constructed for N events, is not a sample of independent values. Therefore, the standard estimates are inapplicable when estimating the confidence intervals [Pisarenko and Pisarenko, 1995]. In the present work, the approximate estimate for the variance of the correlation dimension was obtained using the method of direct estimation (jackknife technique), which is based on the analysis of the statistical function of influence [Sidorin and Smirnov, 1995]. Applying this method, one can assess that part of the uncertainty in the estimate, which is due to the finite sample size.

***q*-value.** The law and the fractal geometry of seismicity reflect the fundamental property of the process of failure, namely, its self-similarity. One can relate the Gutenberg–Richter law to the statistics of the sizes of earthquake sources, because it shows how the number of earthquakes changes as the sizes of earthquake sources change. In the estimation of the correlation dimension, the fractal geometry deals with the distribution of distances between the events: the correlation dimension shows how the number of pairs of events changes as the distance between them changes. Both laws can be combined into a single law known as a generalized Gutenberg–Richter law [Keilis-Borok et al., 1989] or a unified scaling law for earthquakes [Bak et al., 2002]:

$$\log N = -b\log E + d\log L + \log T + \mathrm{const},$$

where N is the number of earthquakes with energy E that occurred in a region of size L within time T. This law incorporates the estimates obtained in different-sized regions for events with different energies, which makes it possible to correctly recalculate the statistics determined in the regions with various sizes.

The unified scaling law provides statistically valid estimates reduced to a region of the size of the earthquake source, which is important for comparing the seismic statistics with the physics of failure that deals with this region. In particular, the duration of the failure cycle of the lithospheric material can be directly estimated from the data provided by the earthquake catalogue [Smirnov, 2003]. The duration of the failure cycle is understood as the time interval inverse to the average frequency of the recurrence of earthquakes in a region of the size of the earthquake source. The average frequency of recurrence in a region of size l is calculated from the average frequency of recurrence in a larger region of size L in which the number of events is sufficient for obtaining statistically valid estimates.

We assume that within time T a region with a size L was hit by n_M earthquakes of magnitude M. We denote the average frequency of earthquake recurrence in this region by $\nu(L) = n_M/T$.. If the earthquakes were uniformly distributed in space, the average frequency of recurrence in a region of size l would be by a factor of $(L/l)^3$ lower: $\nu(l) = \nu(L)\ (l/L)^3$. However, the spatial distribution of earthquakes is actually nonuniform. This nonuniformity is easy to take into account if we assume that the geometry of seismicity is fractal. If the fractal (correlation) dimension is d, one should use $(l/L)^d$ instead of $(l/L)^3$ when calculating $\nu(l)$. In this case, the average duration of the failure cycle $\tau(l) = 1/\nu(l)$ for earthquakes with a source size l is

$$\tau(l) = \tau_0(l/l_0)^q,$$

where τ_0 is the duration of the failure cycle for events with source size l_0, $q = \alpha b - d$. The coefficient α depends on the scale of magnitude used: it governs the relation between the magnitude and the source size $M = \alpha \log l + \beta$. The q-value and τ_0 parameter can be directly estimated from the data of the earthquake catalogue; the technique is described in detail in [Smirnov, 2003].

The q parameter shows how the duration of the cycle of failure depends on the size (or magnitude) of the earthquake source. The results obtained in [Smirnov, 2003] indicate that the duration of the failure cycle in the case of background seismicity only slightly depends on magnitude (q parameter is close to zero). It means that in the undisturbed conditions of background seismicity, the process of failure develops with equal intensity on different scales, which correspond to different sizes of seismic sources. It was supposed in [Smirnov, 2003] that the dependence of the duration of a failure cycle on the size of the earthquake source probably reflects the redistribution of stresses over the hierarchy levels in the system of lithospheric heterogeneities. The fact that q is close to zero means that the heterogeneities of different sizes have an approximately equal probability to fail and, correspondingly, the stress field on long time scales is to some extent consistent with the "field" of strength.

The q-value also reflects the difference in scalings (decay exponents) that characterize the statistical distributions of sizes of the earthquake sources (the exponent is αb) and the distances between the earthquakes (the exponent is d). If these distributions agree with each other, i.e., if the distances between the sources are proportional to their sizes, then $q = 0$ or $b = d/\alpha$. This idea lies behind many studies focusing on the interpretation of statistical properties of the seismic regime [Aki, 1981; King, 1983; Turcott, 1992; Grigoryan, 1988; Smirnov, 1997b; Bak et al., 2002; Corral, 2005].

Investigation of the aftershock sequences and modeling of transient modes of seismicity revealed considerable deviations of the q-parameter from zero and its regular variations in time, which indicate the redistribution of the scale of failure in these cases [Smirnov and Ponomarev, 2004; Smirnov et al., 2010].

Spatial size of a swarm. The effective size of the swarm cloud is estimated in terms of the so-called radius of gyration, which is the root mean square distance of the swarm events from the barycentre, whose coordinates are the average coordinates of earthquakes of the swarm:

$$R_g = \sqrt{\frac{1}{N}\sum_{i=1}^{N}(x_i - X_0)^2 + (y_i - Y_0)^2 + (z_i - Z_0)^2},$$

where X_0, Y_0, and Z_0 are the average coordinates of the events that determine the coordinates of the barycentre.

The radius of gyration has a sense of an estimate of the variance in the Gaussian approximation of the cloud of events. The diameter of gyration $D_g = 2R_g$ defines the area that encompasses approximately 66% (in case of the Gaussian distribution) of the events, and the double diameter of gyration defines the area containing 96% of the events. The latter quantity was used as the estimate of the spatial size of the swarm $L = 2D_g = 4R_g$.

THE RESULTS

The statistical parameters for the swarm of 2001 are presented in Fig. 5 (within the area shown in the first three maps in Fig. 4). The volume of the working catalogue selected by the magnitude of completeness ($M \geq 1.4$) was 1279 events. Estimation was conducted in moving time windows. Each window contained 150 events and was shifted by 15 events. Constraining the length of a window to a certain number of events rather than to a certain time span provided the statistical representativeness of estimates that is constant in

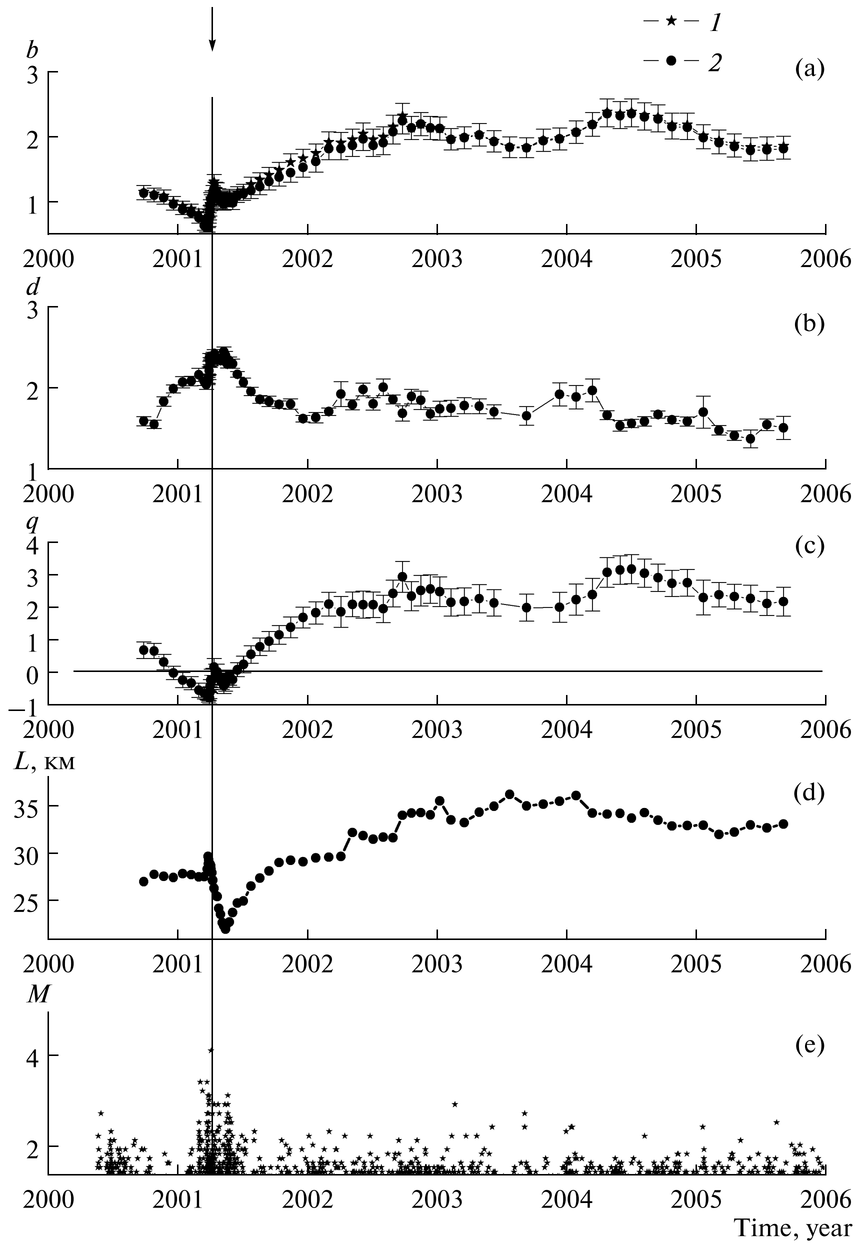

Fig. 5. Time variations of the statistical parameters of seismicity for the swarm of 2001. (a) b-value: *1* estimates on the right, (*2*) estimates on the left; (b) fractal dimension of the set of hypocenters; (c) q-value $q = 2b - d$; (d) swarm size; (e) magnitude of earthquakes. The moment of $M = 4.2$ earthquake of April 8, 2001 is indicated by a vertical line.

time, which is in demand when comparing the estimates for small samples.

The changes in the statistical parameters of the seismic regime associated with swarm activity are clearly manifested in Fig. 5. Figure 6 illustrates these variations on a finer time scale immediately before, during, and after the swarm (this part of the working catalogue, which corresponds to the swarm of 2001, includes 652 events). It can be seen that at the stage of increasing activity the b-value decreases, the fractal dimension of the set of hypocenters d increases, and the size L of the swarm remains almost the same. The q-value (calculated as $q = \alpha b - d$) with $\alpha = 2$, which corresponds to the moment magnitude) decreases and passes from positive to negative values.

At the stage of decay in swarm activity, parameters b, d, and q change in the opposite manner: b increases, d decreases, and q increases, recovering to positive values. The size of swarm L decreases during the swarm activity itself, and then expands up the entire seismogenic region covered by the catalogue.

Variations in the parameters of seismicity for the swarm of 2003–2004 (within the area shown on the last four maps of Fig. 4) are depicted in Fig. 7. It can

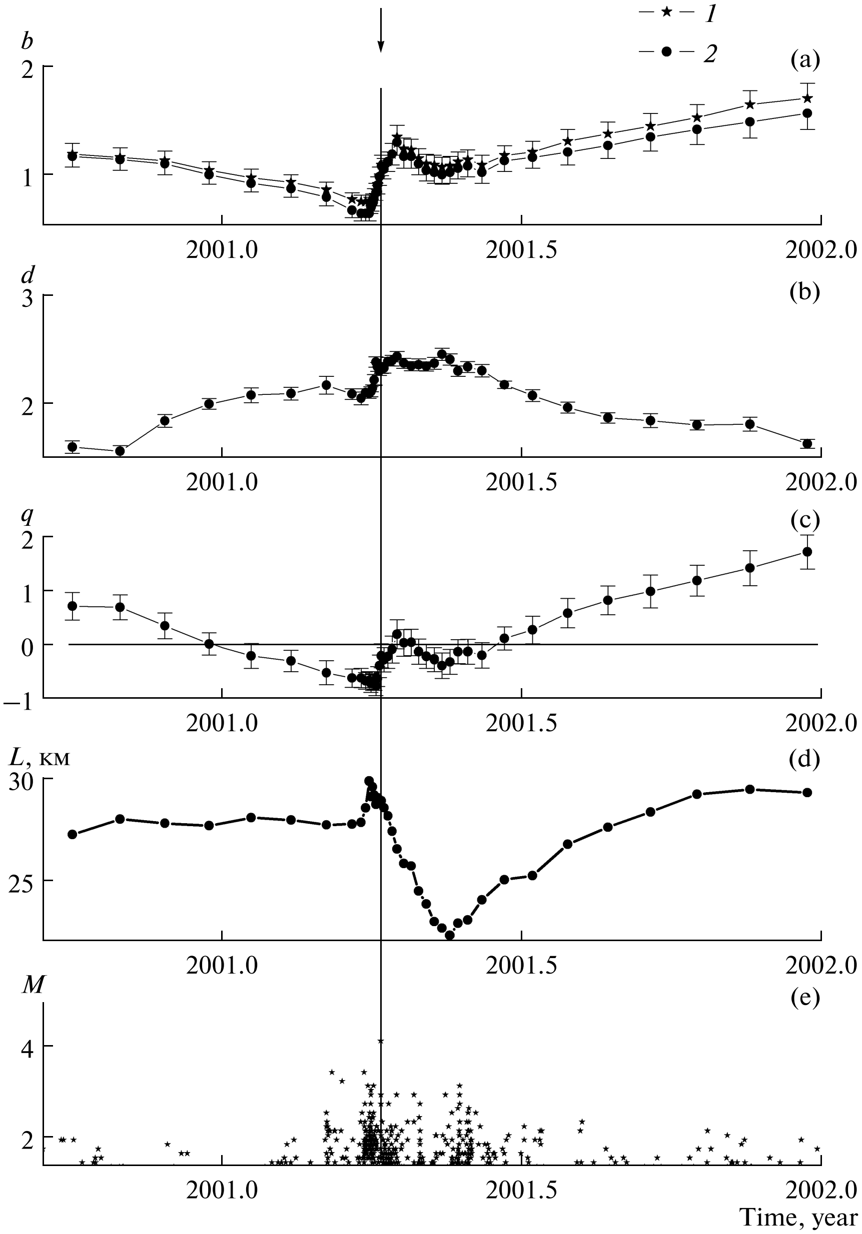

Fig. 6. Time variations of the statistical parameters of seismicity for the swarm of 2001; a detailed view for the interval from October 2000 to 2002. Designations are the same as in Fig. 5.

be seen that as the swarm activity grows, the *b*-value decreases, the fractal dimension *d*-value increases, the *q*-value drops to negative values, and the spatial extent of the swarm reduces. At the stage of decaying activity, these parameters vary inversely.

Figure 8 illustrates variations in the *L*-values calculated for both swarms without overlapping of the time windows. Each point corresponds to 50 events. As the swarm activity increases, the *b*-value exhibits a general trend of a decrease, which is followed by an increase at the stage of activity decay. However, in the swarm of 2001, there are outliers that fall outside the general trend. These points refer to the strong $M = 4.2$ event of April 8, 2001, which is marked by the vertical bold line in Fig. 8a. The interval containing this event is presented on a larger scale in Fig. 9 where the *b*-value was calculated strictly before and after the seismic event of April 8, 2001 (here, in overlapping windows). This strong event evidently interrupts the smooth behavior of the *b*-value. Clearly, in this case, superimposition or some other more complex interaction occurs between the processes of the evolution of the swarm and the source of the earthquake; however, the insufficiently fine level of detail and insufficient volume of the initial data does not allow us to separate these processes and to elucidate the character of this interaction.

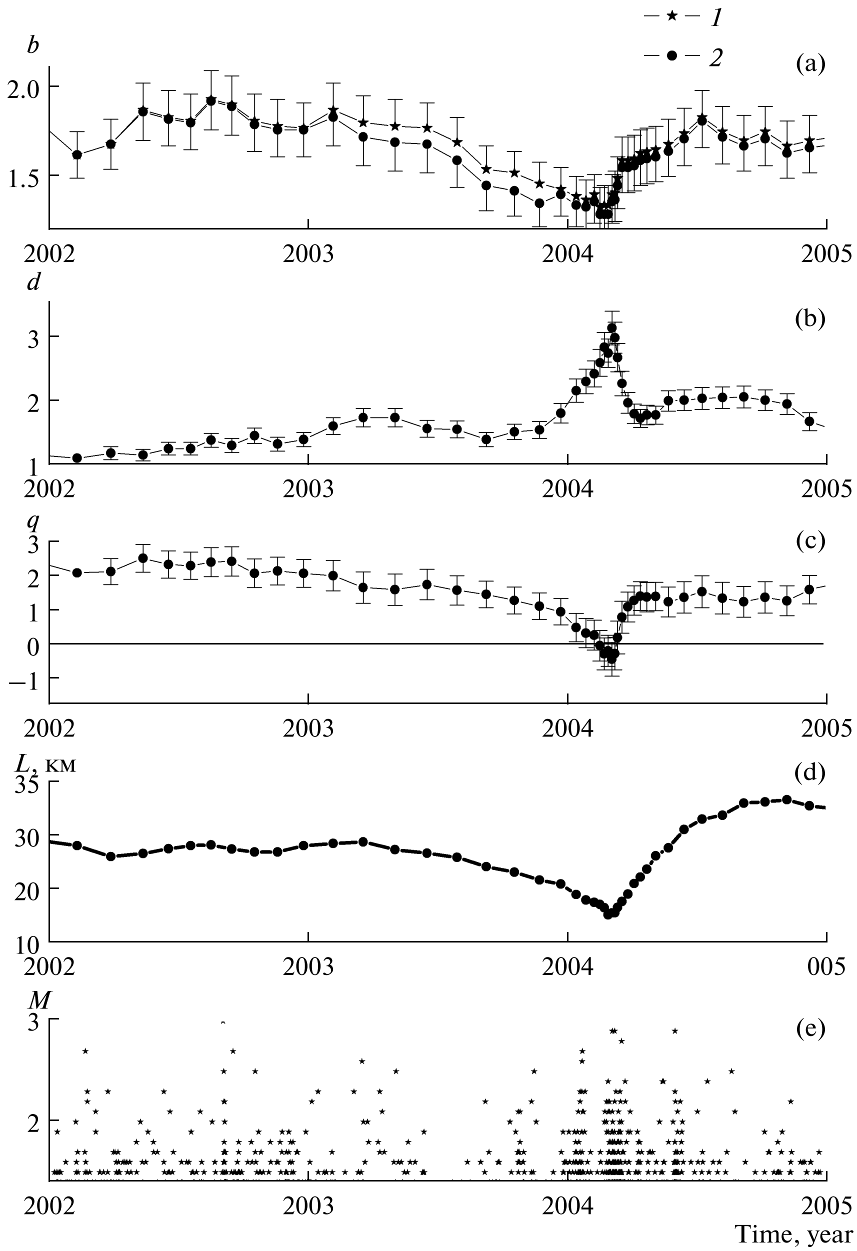

Fig. 7. Time variations of the statistical parameters of seismicity for the swarm of 2003–2004: (a) b-value, (*1*) estimates on the right, (*2*) estimates on the left; (b) fractal dimension of the set of hypocenters; (c) q-value $q = 2b - d$; (d) swarm size; (e) magnitudes of earthquakes.

THE DISCUSSION

For both swarms, the analysis revealed salient changes in the parameters of the seismic regime which reflect the development of swarm activity. These changes indicate that the development of the swarm's activity, just as the evolution of the source zones of earthquakes, is accompanied (and, probably, even governed) by the redistribution of the failure over scales. The decrease in the q-value at the stage of an increase of swarm activity (as well as the decrease in the b-value) indicates that failure gradually passes to increasingly higher levels: the decrease in the q-value means a shortening of the failure cycle for larger sources compared to smaller sources. This corresponds to the scenario of the so-called inverse cascade, i.e., to the transfer of a failure from smaller to larger scales. Such a scenario is typical for the preparation of the source zones of earthquakes and is known as the AUF (avalanche unstable fracture) scenario, or the scenario of crack fusion and growth [Sobolev, 1993]. At the stage of decay of the swarm activity, the q-value (as well as b-value) increases, which indicates the redistribution of the failure from larger to smaller

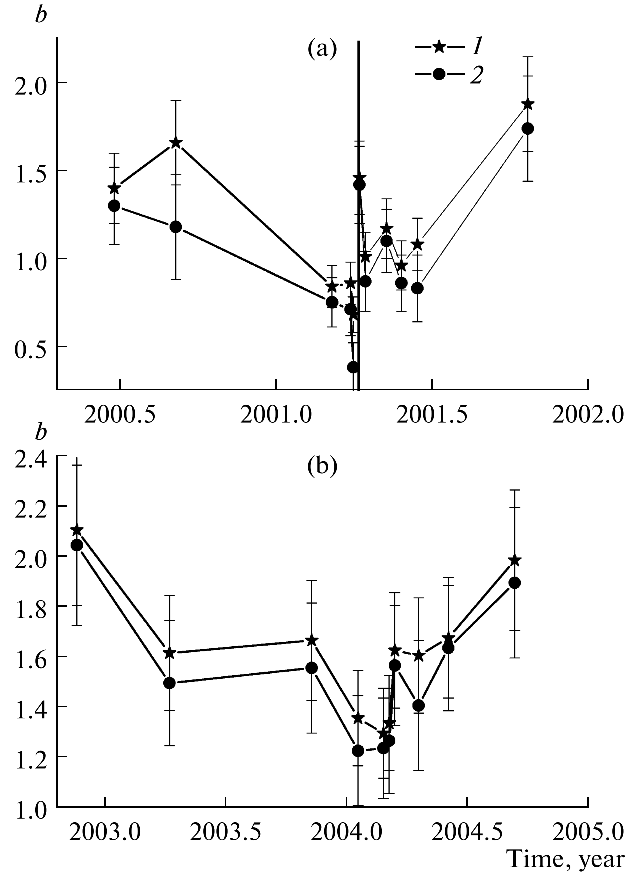

Fig. 8. Variations of b-value within non-overlapping time windows. (a) the swarm of 2001; (b) the swarm of 2003–2004. (*1*) the estimate on the right, (*2*) the estimate on the left.

scales (a direct cascade). This scenario is rendered in the aftershock sequences [Smirnov and Ponomarev, 2004].

Thus, the trends in the seismic regimes of the swarms studied are qualitatively similar to the scenarios of the preparation and "after-action" of the sources of earthquakes. The quantitative discrepancy in the development of a swarm and an earthquake source zone can be recognized in the rate of evolution of the inverse cascade. During the preparation of the earthquake source, at least at its final stage, the inverse cascade develops with acceleration, assuming an avalanche-like character. The reason why a similar progression of failure in one case culminates in a swarm while in another case it is terminated by a strong earthquake remains unclear.

Based on the hypothesis of the similarity in the development of swarms and earthquake sources, we can propose an explanation to the anomaly in the variations of the b-value shown in Fig. 9. If similarity is the case, the curve in Fig. 9 can be considered as a superimposition of a curve reflecting the decrease/increase in the b-value that is due to the development of a swarm (like the curve shown in Fig. 8b) and another curve of the decrease/increase in the b-value caused by the preparation and relaxation of the source of earthquake on April 8, 2001. If the time span of the latter curve is less than that of the former one, and the time moment of the earthquake does not coincide with the transition of the swarm activity from enhancement to decay, then the superimposition of the curves will result in exactly what is shown in Fig. 9. In other

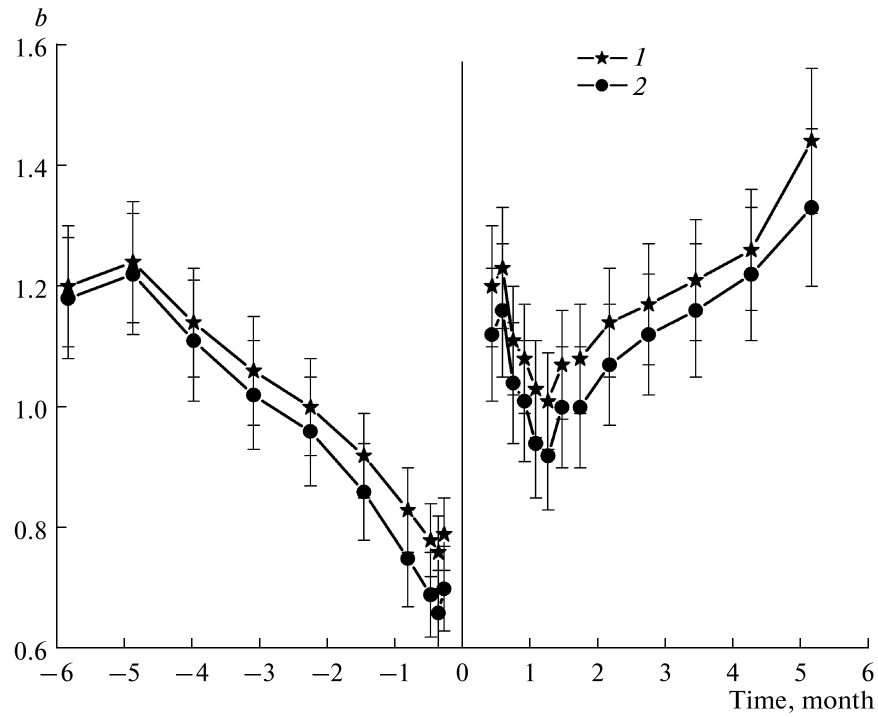

Fig. 9. Variations of b-value for the swarm of 2001 before and after the earthquake of April 8, 2001. Time is measured from the earthquake origin time. (*1*) the estimate on the right, (*2*) the estimate on the left.

words, the anomaly in the b-value after the earthquake of April 8, 2001 should be regarded as a consequence of the increase in the b-value, which is typical for the aftershock's relaxation. This explanation is only a hypothesis, because the swarm and the earthquake of April 8, 2001 are treated as independent events, which has not been substantiated in the present work. Elucidation of this question requires, as mentioned above, the use of more detailed initial data.

The trends in the development of seismic swarms in the Corinth rift, which are revealed in the present work, are similar (in terms of the pattern of changes in the seismic regime) to the results obtained in the laboratory and field experiments [Smirnov et al., 2010]. To some extent, this confirms the conclusion about a universal scenario of development of the transient regimes in seismicity. Here, it should be noted that the mode of initiation of seismic activity in these experiments was different from that of the swarms considered. In the experiments (both the laboratory and field experiment), seismicity has been initiated by increasing the stresses (in the laboratory, by the action of a press, and in the field experiment, by increasing the pressure of water injected into a borehole). The origin of swarms in the Corinth rift is believed not to be related, at least directly, to significant changes in the crustal stresses. When considering the probable reason for the appearance of swarms, a certain fluid diffusion in the upper portions of the crust is meant; both deep and surface (due to precipitation) origins of the fluid are assumed possible [Bourouis and Cornet, 2009]. Such an initiation should probably not be considered as a change in the state of the medium but rather as a change in the properties of the medium, namely, a decrease in strength. The similarity in the evolution of transient modes of seismicity initiated by different influences supports the idea of a universal mechanism responsible for these seismic processes.

CONCLUSIONS

1. The changes in the parameters of seismicity during the periods of swarm activity in 2001 and 2003-2004 in the Corinth rift indicate that the process of failure exhibits redistribution over scales over the course of time. The stage of increasing activity is accompanied by progression from smaller to larger scales, while the stage of decay, by evolution from larger to smaller scales. These features of excitation and relaxation of swarm activity are qualitatively similar to the scenarios of source preparation and aftershock relaxation of an earthquake.

2. The swarm of 2001 differed from the swarm of 2003–2004 by the occurrence of a relatively strong $M = 4.2$ earthquake on April 8, 2001. This earthquake introduced a perturbation in the seismic regime; however, it did not violate the general trend in the variations of the parameters of swarm activity.

3. The pattern of changes in the parameters characterizing the seismic regime of the swarms studied is similar to the variations in these parameters revealed in the previous laboratory and field models of various transient processes. This confirms the validity of the results and conclusions of the experimental investigations of the transient modes of seismicity and indicates that the mechanism responsible for them is universal.

ACKNOWLEDGMENTS

We are grateful to A.V. Ponomarev for his useful discussion of the obtained results. The work was carried out under the program of scientific collaboration between the Schmidt Institute of Physics of the Earth and Institute de Physique du Globe de Paris (France). The research was supported by the Russian Foundation for Basic Research, grants 09-05-91056-NTsNI and 11-05–00135.

REFERENCES

Aki, K. Probabilistic Synthesis of Precursory Phenomena in Earthquake Prediction, in *Earthquake Prediction: An International Review,* Simpson, D. W. and Richards, P. G., Eds., Washington D.C.: Am. Geophys. Un., 1981, pp. 556–574.

Avallone, A., Briole, P., Agatza-Balodimou, A.M., et al., Analysis of Eleven Years of Deformation Measured by GPS in the Corinth Rift Laboratory Area, *C. R. Geosci.,* 2004, vol. 336, pp. 301–312.

Bak, P., Christensen, K., Danon, L., and Scanlon, T., Unified Scaling Law for Earthquakes, *Phys. Rev. Lett.,* 2002, vol. 88, no. 17, DOI: 10.1103/PhysRevLett.88.178501.

Bell, R., McNeill, L., Bull, J., et al., Fault Architecture, Basin Structure and Evolution of the Gulf of Corinth Rift, Central Greece, Basin Research, 2009, vol. 21, no. 6, pp. 824–855, doi: 10.1111/j.1365-2117.2009.00401.x.

Bernard, P., Briole, P., Meyer, B., et al. The M_s=6.2, June 15, 1995 Aigion Earthquake (Greece): Evidence for Low-Angle Normal Faulting in the Corinth Rift, *J. Seismol.,* 1997, vol. 1, pp. 131–150.

Bernard, P., Lyon-Caen, H., Briole, P., et al. Seismicity, Deformation and Seismic Hazard in the Western Rift of Corinth: New Insights from the Corinth Rift Laboratory (CRL), *Tectonophys.,* 2006, vol. 426, nos. 1–2, pp. 7–30.

Bourouis, S. and Cornet, F. H. Microseismic Activity and Fluid Fault Interactions: Some Results from the Corinth Rift Laboratory (CRL), Greece, *Geophys. J. Int.,* 2009, vol. 178, no. 1, pp. 561-–580.

Briole, P., Rigo, A., Lyon-Caen, H., et al., Results from Repeated Global Positioning System Surveys between 1990 and 1995, *J. Geophys. Res.,* 2005, vol. 105, pp. 25605–25 625.

Corral, A., Renormalization-Group Transformations and Correlations of Seismicity, *Phys. Rev. Lett.,* 2005, vol. 95, DOI: 10.1103/PhysRevLett.95.028501.

Feder, J., Fractals, New York, Plenum Press, 1988.

Ford, M., Williams, E. A., Malartre, F. and Popescu, S.-M. Stratigraphic Architecture, Sedimentology and Structure of the Vouraikos Gilbert-Type Fan Delta, Gulf of Corinth, Greece, in *Sedimentary Processes, Environments and Basins:*

A Tribute to Peter Friend, Nichols, G., Williams, E. and Paola, C., Oxford, UK: Wiley-Blackwell, 2007, pp. 44–90, doi: 10.1002/9781444304411.ch4.

Grigoryan, S.S., On the Mechanism of Earthquake Generation and the Meaning of Empirical Laws in Seismology, *Dokl. Akad. Nauk SSSR,* 1988, vol. 299, no. 5, pp. 235–240.

Henry, P. and Moretti, I., The Understanding of Fault Activity from Natural Laboratories, *Tectonophys.,* 2006, vol. 426, nos. 1–2, pp. 1–5.

Keilis-Borok, V.I., Kossobokov, V.G., and Mazhkenov, S.A., On a Similarity in Spatial Distribution of Seismicity, *Vychislitel'naya seismologiya,* 1989, no. 22, pp. 28–40.

Kendall, M.G. and Stuart, A., *The Advanced Theory of Statistics,* vol. 2: *Inference and Relationship,* New York: Hafner Publishing Company, 1961.

King, G., The Accommodation of Large Strain in the Upper Lithosphere of the Earth and Other Solids by Self-Similar Fault System: the Geometrical Origin of b-Value, *Pure Appl. Geophys.,* 1983, vol. 121, pp. 761–815.

Lykoussis, V., Sakellariou, D., Moretti, I., and Kaberi, H., Late Quaternary Basin Evolution of the Gulf of Corinth: Sequence Stratigraphy, Sedimentation, Fault Slip and Subsidence Rates, *Tectonophys.,* 2007, vol. 440, nos. 1–4, pp. 29–51, doi: 10.1016/j.tecto.2006.11.007.

Lyon-Caen, H., Papadimitriou, P., Deschamps, A., et al., First Results of CRLN Seismic Array in the Western Corinth Rift: Evidence for Old Fault Reactivation, *C. R. Geosci.,* 2004, vol. 336, nos. 4–5, pp. 343–351.

Mandelbrot, B.B., *The Fractal Geometry of Nature,* New York: W.H. Freeman and Co., 1982.

McNeill, L.C., Collier, R.E.L., De Martini, P. M., et al., Recent History of the Eastern Eliki Fault, Gulf of Corinth: Geomorphology, Paleoseismology and Impact on Paleoenvironments, *Geophys. J. Int.,* 2005, vol. 161, pp. 154–166.

Pacchiani, F. and Lyon-Caen, H., Geometry and Spatio-Temporal Evolution of the 2001 Agios Ioanis Earthquake Swarm (Corinth Rift, Greece), *Geophys. J. Int.,* 2010, vol. 180, no. 1, pp. 59–72, doi: 10.1111/j.1365-246X.2009.04409.x.

Pisarenko, D.V. and Pisarenko, V.F., Statistical Estimation of the Correlation Dimension, *Phys. Lett.,* 1995, vol. A197, pp. 31–39.

Pisarenko, V.F., On a Law of Earthquake Recurrence, in *Diskretnye svoistva geofizicheskoi sredy* (Discrete Properties of a Geophysical Medium), Moscow: Nauka, 1989, pp. 47–60.

Rietbrock, A., Tiberi, C., Sherbaum, F., and Lyon-Caen, H., Seismic Slip on a Low Angle Normal Fault in the Gulf of Corinth: Evidence from High Resolution Cluster Analysis of Microearthquakes, *Geophys. Res. Lett.,* 1996, vol. 23, no. 14, pp. 1817–1820.

Rigo, A.A., Lyon-Caen, H., Armijo, R., et al., A microseismic Study in the Western Part of the Gulf of Corinth (Greece): Implications for Large Scale Normal Faulting Mechanisms, *Geophys. J. Int.,* 1996, vol. 126, pp. 663–688.

Sadovskii, M.A. and Pisarenko, V.F., *Seismicheskii protsess v blokovoi srede* (Seismic Process in a Block Medium), Moscow: Nauka, 1991.

Sidorin, I.A. and Smirnov, V.B., Changeability of Correlation Dimension Due to Heterogeneity of a Fractal (Case Study of the Lorenz Attractor), *Fiz. Zemli,* 1995, no. 7, pp. 89–96.

Smirnov, V. B., Ponomarev, A. V., and Zav'yalov, A.D., The Structure of Acoustic Regime in Rock Samples and the Seismic Process, *Fiz. Zemli,* 1995, no. 1, pp. 38–58.

Smirnov, V.B., Experience of Estimating the Completeness of Earthquake Catalogues, *Vulkanologiya i seismologiya,* 1997a, no. 4, pp. 93–105.

Smirnov, V.B., Spatial and Temporal Variations in the Self-Similarity Indices of Seismicity, *Vulkanologiya i seismologiya,* 1997b, no. 6, pp. 31–41.

Smirnov, V. B. and Feofilaktov, V.D., Fractal Properties of the Lithosphere According to Coda Waves from Local Earthquakes and the Structure of Seismicity in the Source Zone of Rachinsk Earthquake, *Vulkanologiya i seismologiya,* 2000, no. 6, pp. 44–48.

Smirnov, V.B., Estimating the Duration of the Lithospheric Failure Cycle from Earthquake Catalogs, *Fiz. Zemli,* 2003, no. 10, pp. 13–32 [*Izv. Phys. Earth* (Engl. Transl.), 2003, vol. 39, no. 10, pp. 794–811].

Smirnov, V.B. and Ponomarev, A.V., Seismic Regime Relaxation Properties from In Situ and Laboratory Data *Fiz. Zemli,* 2004, no. 10, pp. 26–36 [Izv. Phys. Earth (Engl. Transl.), 2004, vol. 40, no. 10, pp. 807–816].

Smirnov, V.B., Ponomarev, A.V., Bernard, P., and Patonin, A.V., Regularities in Transient Modes in the Seismic Process according to the Laboratory and Natural Modeling, *Fiz. Zemli,* 2010, no. 2, pp. 17–49 [*Izv. Phys. Earth* (Engl. Transl.), 2010, vol. 46, no. 10, pp. 104–135].

Sobolev, G.A., *Osnovy prognoza zemletryasenii* (Principles of Earthquake Prediction), Moscow: Nauka, 1993.

Sobolev, G.A., Arora, B., Smirnov, V.B., et al., Prognostic Anomalies of Seismic Regime: 2. Western Himalaya, *Geofizicheskie Issledovaniya,* 2009, vol. 10, no. 2, pp. 23–36 [*Izv. Phys. Earth (*Engl. Transl.), 2009, vol. 10, no. 2, pp.?23–36].

Turcotte, D.L. *Fractals and Chaos in Geology and Geophysics,* Cambridge: Cambridge Univ. Press, 1992.